

# Why Do Nitroso Compounds Dimerize While Their Oxime Tautomers Do Not? A Structural Study of the *Trans*-Dimer of 2-Chloro-2-methyl-3-nitrosobutane and Higher Level *ab Initio* Study of Thermodynamic Stabilities and Electronic Structures of Isomers of Diazene Dioxides

Rainer Glaser,\* R. Kent Murmann,\* and Charles L. Barnes

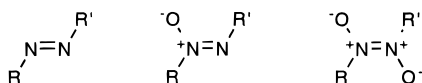
Department of Chemistry, University of Missouri—Columbia, Columbia, Missouri 65211

Received April 25, 1995<sup>®</sup>

NOCl addition to 2-methyl-2-butene produces a white crystalline solid which was shown by low-temperature X-ray diffraction to contain *trans*-dimers **2** of 2-chloro-2-methyl-3-nitrosobutane (**1n**): C<sub>10</sub>H<sub>20</sub>N<sub>2</sub>O<sub>2</sub>Cl<sub>2</sub>, *M<sub>r</sub>* = 271.18, monoclinic, *I*2/a, *a* = 11.982(4), *b* = 7.1297(7), *c* = 15.735(5) Å, β = 90.20(2)°, *V* = 1344.2(6) Å<sup>3</sup>, *Z* = 4, *D<sub>x</sub>* = 1.340(2) g cm<sup>-3</sup>, (Mo Kα) = 0.70930 Å, μ = 4.7 cm<sup>-1</sup>, *F*(000) = 1152, *T* = 173 K, *R* = 0.030, *R<sub>w</sub>* = 0.032 for 791 observed reflections of 898 unique data. Diazene dioxide **2** also is the dominant species in solution although some spectroscopic and chemical observations indicate the presence of monomeric nitroso compound **1n** and of the tautomeric oxime **1o** at least in small quantities. In conjunction with the experimental study, conformational and configurational equilibrium structure preferences and the bonding in diazene dioxides R(O)NN(O)R' (**3**: R = R' = H, **4**: R = H, R' = Me, **5**: R = R' = Me) were studied at the MP2(full)/6-31G\* level. The <sup>1</sup>A' and <sup>3</sup>A' states of HNO and MeNO and the oxime tautomer of MeNO were considered. Isomer energies, rotational barriers, excitation energies, tautomerization energies, and dimer formation energies were determined at levels up to QCISD(T)/6-311G\*\*//MP2(full)/6-31G\* + ΔVZPE-(MP2(full)/6-31G\*). The *trans*-isomer is favored in all cases, and the *trans* preference energy increases from 4.0 kcal/mol in (HNO)<sub>2</sub> to 13.2 kcal/mol in (MeNO)<sub>2</sub>. The thermodynamic stabilities of the *trans*-configured diazene dioxides vary by less than 1 kcal/mol as the result of successive H/Me replacement; the calculated dimerization enthalpies for the *trans*-isomers are -9.0 (**3**), -9.9 (**4**), and -9.4 kcal/mol (**5**). Natural bond orbital analysis and dipole and quadrupole moments show dimer formation to increase the polarity of the NO bond, and this increase is only slightly larger for the Me-substituted NO bond. *The driving force for dimer formation is the electron density transfer to the most electronegative element and this density transfer is made possible by N-rehybridization.* The analogous dimerization of oximes via N<sub>o</sub> lone pair [2 + 2] addition would result in an unfavorable polarization reversal for the C-atom.

## Introduction

Diazene dioxides result from NN connection of nitroso compounds and may be considered the highest oxidized species in the series diazene, azoxy, and dioxidiazene. The crystallographic record contains reports on diazene dioxides with aromatic and aliphatic groups,<sup>1</sup> R and R',



while some nitroso compounds exist as monomers in the solid state.<sup>2</sup> For dimeric nitrosomethane both the *cis* and *trans* isomers were isolated and studied crystallographically.<sup>3</sup> The oxygens are arranged in a *trans* fashion<sup>4</sup> in

most cases and less frequently in the *cis* fashion<sup>5</sup> unless such a configuration is forced by rings.<sup>6</sup> Isomerization can be accomplished in some cases photochemically.<sup>7</sup> The formation of diazene dioxides might also occur with some oximes which can tautomerize into the nitroso form. In particular, we will be concerned here with the nitroso-

(4) *Trans* diazene dioxides: (a) *p*-Bromonitrosobenzene dimer: Darwin, C.; Hodgkin, D. C. *Nature* **1950**, *166*, 827. (b) 2,4,6-Tribromonitrosobenzene dimer: Fenimore, C. P. *J. Am. Chem. Soc.* **1950**, *72*, 3226. (c) *Trans* dimer of 2-nitronitrosoethane: Boer, F. P.; Turley, J. W. *J. Am. Chem. Soc.* **1969**, *91*, 1371. (d) *Trans* dimer of nitrosocyclohexane: Tanimura, M.; Kobori, K.; Kashiwagi, M.; Kinoshita, Y. *Bull. Chem. Soc. Jpn.* **1970**, *43*, 1962. (e) *trans*-2,2'-Dicarboxyazobenzene dioxide: Dieterich, D. A.; Paul, I. C.; Curtin, D. Y. *J. Am. Chem. Soc.* **1974**, *96*, 6372. (f) (*E*)-1,2-Bis(1-nitro-1-methylethyl)diazene 1,2-dioxide: Tinant, B.; Declercq, J. P.; Exner, O. *Bull. Soc. Chim. Belg.* **1987**, *96*, 149. (g) *Trans*-dimeric 2-methyl-2-nitrosopropane: Gowenlock, B. G.; McCullough, K. J.; Manson, R. B. *J. Chem. Soc., Perkin Trans. 2* **1988**, 701. (h) *trans*-2,2',6,6'-tetraisopropylazodioxibenzene: Gowenlock, B. G.; McCullough, K. J. *J. Chem. Soc., Perkin Trans. 2* **1989**, 551. (i) For detailed <sup>1</sup>H- and <sup>13</sup>C-NMR studies of monomeric 2-chloro-2-nitrosobornane and its diastereoisomeric *trans*-diazene dioxide dimers, see: Boucenna, M.-C.; Davidson, J. S.; McKee, A.; Porte, A. L.; Apperley, D. C. *J. Chem. Soc. Perkin Trans. 2* **1995**, 1381–1387. (j) *trans*-*N,N*-dioxo-1,1'-azobis(norbornane): Greer, M. L.; Sarker, H.; Mendicino, M. E.; Blackstock, S. C. *J. Am. Chem. Soc.* **1995**, *117*, 10460–10467.

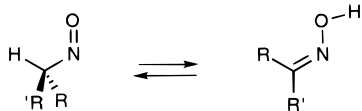
(5) *Cis* diazene dioxides: (a) *cis*-azobenzene dioxide: Dieterich, D. A.; Paul, I. C.; Curtin, D. Y. *J. Am. Chem. Soc.* **1974**, *96*, 6372. (b) *Cis* dimer of pentafluoronitrosobenzene: Prout, C. K.; Coda, A.; Forder, R. A.; Kamenar, B. *Cryst. Struct. Commun.* **1974**, *3*, 39.

<sup>®</sup> Abstract published in *Advance ACS Abstracts*, December 15, 1995.

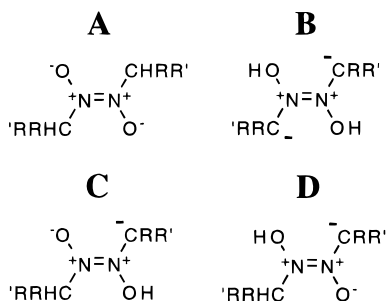
(1) Allman, R. Structural Chemistry. In *The Chemistry of the Hydrazo, Azo, and Azoxy Groups*; Patai, S., Ed., John Wiley & Sons: New York, 1975; Chapter 2, Part 1, p 49ff.

(2) (a) *N,N*-dimethyl-*p*-nitrosoaniline monomer: Rømming, C.; Talberg, H. J. *Acta Chem. Scand.* **1973**, *27*, 2246. (b) (+)-10-Bromo-2-chloro-2-nitrocyclohexane: Ferguson, G.; Fritchie, C. J.; Robertson, J. M.; Sim, G. A. *J. Chem. Soc.* **1961**, 1976–1987.

(3) X-ray structures of nitrosomethane dimer: (a) *cis*: Germain, G.; Piret, P.; Meerssche, M. van. *Acta Crystallogr.* **1963**, *16*, 109. (b) *trans*: Meerssche, M. van; Germain, G. *Bull. Soc. Chim. Belg.* **1959**, *68*, 244.



oxime tautomerization between 2-chloro-2-methyl-3-nitrosobutane ( $R = \text{Me}$ ,  $R' = \text{CMe}_2\text{Cl}$ ), **1n**, and 2-chloro-2-methylbutanone 3-oxime, **1o**, which has been utilized in the preparation of  $\alpha$ -amine oximes. These  $\alpha$ -amine oximes are excellent chelating agents for small transition metal ions in their lower oxidation states<sup>8,9</sup> and have unique significance as ligands in brain imaging.<sup>10a,b</sup> Moreover, quasiaromatic  $d^8$ -molecules<sup>10c</sup> with these ligands have potential as photoelectric materials.<sup>10d</sup> It is for these reasons that studies of the structural nature and of the interesting bonding situation in dimers of nitrosoalkanes have become increasingly desirable. In this context, we have performed a structural study of **1** in the solid state and in solution. X-ray structure analysis established its dimeric *trans* configured diazene dioxide structure **2** as opposed to a potentially occurring oxime structure. The NN connected dimers **A** exist while none of the tautomeric dimers **B–D** or of their geometrical isomers<sup>11</sup> apparently are known in this or any other case.



Dimers **B** formally might result by NN connection of two oximes. Tautomers of type **C** can be seen as resulting by NN connection of a nitroso compound with its oxime tautomer. Tautomer **D** can be viewed as the imino *N*-oxide of an *N*-hydroxylated hydrazone. One might wonder why isomers **A** exist while apparently none of the tautomers **B–D**—which contain at least one oxime fragment  $\text{RR}'\text{C}=\text{NOH}$  or an oxime anion  $\text{RR}'\text{C}=\text{NO}^-$ —has ever been described. We will provide an answer to this question using modern ab initio methods.

(6) *Cis* diazene dioxides in ring systems: (a) 1,8-Dinitrosonaphthalene: Prout, C. K.; Cameron, T. S.; Dunn, R. M. A.; Hodder, O. J. R.; Viterbo, D. *Acta Crystallogr. B* **1971**, *27*, 1310. (b) *cis*-Azodiquinoxaline dioxide: Armand, J.; Armand, Y.; Boulares, L.; Philoche-Levisalles, M.; Pinson, J. *Can. J. Chem.* **1981**, *59*, 1711. (c) 2,3-Diazabicyclo[2.2.1]hept-2-ene 2,3-dioxide, 3,3,4,4-tetramethyldiazetidene 1,2-dioxide, 6,7-diazatetracyclo-[3.2.1.1<sup>3,8</sup>.0<sup>2,4</sup>]non-6-ene 6,7-dioxide: Prout, K.; Stothard, V. P.; Watkin, D. J. *Acta Crystallogr., Sect. B* **1978**, *34*, 2602. (d) 1,3,4-Trifluoro-7,9-dimethyl-11*H*-pyrido[4,3-*c*][1,2]benzodiazepine 5,6-dioxide: Banks, R. E.; Djebli, Y.; Fields, R.; Olawore, N. O.; Pritchard, R. G.; Tsiliopoulos, E.; Mason, J. *J. Chem. Soc., Perkin Trans. 1* **1989**, 1117.

(7) Morrison, H. A. *The Photochemistry of the Nitro and Nitroso Groups*. In *The Chemistry of the Nitro and Nitroso Groups*; Feuer, E., Ed., John Wiley & Sons: New York, 1969; Chapter 4, Part 1, p 165. (8) Murmann, R. K. *J. Am. Chem. Soc.* **1957**, *79*, 521.

(9) Siripaisarnpipat, S.; Schlemper, E. O. *Inorg. Chem.* **1983**, *22*, 282.

(10) (a) Fair, C. K.; Troutner, D. E.; Schlemper, E. O.; Murmann, R. K.; Hoppe, M. L. *Acta Crystallogr.* **1984**, *C40*, 1544. (b) Troutner, D. E.; Volkert, W. A.; Hoffman, T. J.; Holmes, R. A. *Int. J. Radiat. Isot.* **1984**, *35*, 467. (c) Murmann, R. K.; Vassian, E. G. *Coord. Chem. Rev.* **1990**, *105*, 1. (d) Murmann, R. K., unpublished results.

(11) We recognize that dimer formations might involve N or O addition to the oxime C=N carbon, that bis-zwitterionic structures **A–C** might close to four-membered ring systems, and so on. We focus here on the tautomeric NN connected noncyclic systems **A–D**.

Theoretical studies have been primarily concerned with the tautomerism of the parent system, HNO versus NOH, and the singlet–triplet splittings. The 1979 configuration interaction (CI) study by Bruna and Marian<sup>12</sup> showed that HNO has a singlet ground state  $^1A'$  and that the triplet state  $^3A''$  is 15.7 kcal/mol less stable while the isomer NOH, hyponitrous acid, is paramagnetic with the  $^3A''$  state being 20 kcal/mol more stable than the  $^1A'$  state. The triplet ground state of NOH is 23.2 kcal/mol above the  $^1A'$  ground state of HNO. Sengupta and Chandra<sup>13</sup> recently discussed these isomers at the MP4sdtq/6-311G\*\*//MP2(full)/6-311G\*\* level and considered the isomerization in both states as well as several decomposition pathways. In their study of the NO addition to HNO, Mebel, Morokuma, Lin, and Melius<sup>14</sup> also considered HNO and NOH at levels up to QCISD(T)/6-311G\*\*/MP2(full)/6-311G\*\*. Schatz, et al.<sup>15</sup> employed CASSCF theory in their study of the global potential energy surfaces of several states of these isomers. It has long been known<sup>16</sup> that NOH exists as the dimer  $\text{HON}=\text{NOH}$  with the *trans*-azo structure. Similarly, the formation of dimers from nitroso compounds had been postulated even before this century.<sup>17</sup> The first theoretical study of diazene dioxides was presented by Hoffmann, Gleiter, and Mallory<sup>18</sup> in 1970. Extended Hückel calculations were used as the basis to discuss the non-least-motion paths for the dimerizations of  $\text{CH}_2$  and HNO. Heiberg<sup>19</sup> studied the least motion dissociation path of the *trans* dimers of MeNO with a limited nonconventional CI approach including geometry optimizations. Minato, Yamabe, and Oda<sup>20</sup> studied the *cis/trans* isomerization of the MeNO dimer using state correlation diagrams, Mulliken populations, and dipole moments determined at the RHF/4-31G level. In 1994, Shancke, et al.<sup>21</sup> studied the isomer preference and formation energies of HNO dimer based on structures optimized at the HF, MP2(full), and QCISD levels and using the 6-31G\* basis set. At all levels, a *trans* preference energy of about 5–6 kcal/mol was found. The dimerization energies were estimated to be –15.0, –8.8, and –16.4 kcal/mol, respectively, at the MP4sdtq/6-31G\*\*//MP2(full)/6-31G\*+ZPE, QCISD(T)/6-31G\*\*//QCISD/6-31G\*+ZPE and G1 levels.

Historically, several resonance forms were considered for the description of the diazene dioxides and, to quote Boer and Turley,<sup>4c</sup> the various proposals caused “some lively discussion” in the literature. Contributions from the canonical forms were discussed primarily on the basis of the structural parameters determined by X-ray crystallography. This methodology suffers from the well recognized fact that such judgments depend on reference

(12) Bruna, P. J.; Marian, C. M. *Chem. Phys. Lett.* **1979**, *67*, 109, and references cited there.

(13) Sengupta, D.; Chandra, A. K. *J. Chem. Phys.* **1994**, *101*, 3906.

(14) Mebel, A. M.; Morokuma, K.; Lin, M. C.; Melius, C. F. *J. Phys. Chem.* **1995**, *99*, 1900.

(15) Guadagnini, R.; Schatz, G. C.; Walch, S. P. *J. Chem. Phys.* **1995**, *102*, 774.

(16) (a) Mason, J.; Bronswijk, W. v. *J. Chem. Soc. A* **1971**, 791, and references cited therein. (b) For a recent reference on hyponitrite chemistry, see: Caldwell, S. E.; Porter, N. A. *J. Am. Chem. Soc.* **1995**, *117*, 8676–8677, and references cited therein.

(17) Tilden, W. A. *J. Chem. Soc.* **1875**, 28, 514.

(18) Hoffmann, R.; Gleiter, R.; Mallory, F. B. *J. Am. Chem. Soc.* **1970**, *92*, 1461.

(19) (a) Heiberg, A. B. *Chem. Phys.* **1977**, *26*, 309. (b) *Ibid.* **1979**, *43*, 415.

(20) Minato, T.; Yamabe, S.; Oda, H. *Can. J. Chem.* **1982**, *60*, 2740.

(21) (a) Lüttke, W.; Shancke, P. N.; Traetteberg, M. *Theor. Chim. Acta* **1994**, *87*, 321, and references cited therein. (b) This article presents a well written and concise history of studies of the diazene dioxide formation.

structural parameters.<sup>22</sup> An alternative approach to electronic structure examination, and the one taken here, consists in the direct analysis of the ground state electron density distributions. In the theoretical part of this article, we report the results of an analysis of the electronic structure of diazene dioxides R(O)NN(O)R' (**3**: R, R' = H, **4**: R = H, R' = Me, **5**: R, R' = Me) in relation to the electronic structures of the singlet and triplet states of the fragments RNO. The effects of the nature of the R group on geometries and NN bond stabilities are discussed in light of the substituent effects on electronic structures. Complete structure optimizations, vibrational, and thermochemical analyses were carried out for **3–5** at higher levels of ab initio theory including modern electron correlation treatments. Comparisons to experimental data (structures, binding energies, dipole moments) were made whenever possible. The electronic structures are discussed based on natural bond orbital (NBO) atomic charges and molecular dipole and quadrupole moments. The insights gained suggest a simple explanation as to why nitroso compounds form such dimers whereas the tautomeric oximes have never been observed to undergo an analogous dimerization.

### Experimental and Theoretical Methods

**X-Ray Crystallography.** Mounting crystals on a glass fiber using epoxy cement was unsuccessful due to the reactivity of the adhesive. The crystals sublimed slowly in air at room temperature. Mounting was accomplished utilizing Apiezon-M grease followed by lowering and maintaining the temperature at  $-100\text{ }^{\circ}\text{C}$  with a T-controlled nitrogen stream. Under these conditions neither movement nor decomposition were noted during data collection as evidenced by the constant intensities of three standard reflections. The crystal used for the X-ray study on the Enraf-Nonius CAD-4 diffractometer was a colorless thick rod,  $0.15 \times 0.2 \times 0.3\text{ mm}$ .

Twenty-five standard reflections with  $10 < \theta < 15^{\circ}$ , Mo  $K_{\alpha}$ , were used to define and refine the cell constants. The space group was determined from systematic absences ( $hkl$ ,  $h+k+l = 2n$ ;  $h0l$ ,  $h,l = 2n$ ). Data was collected up to  $2\theta_{\text{max}} = 46^{\circ}$  ( $-13 \leq h \leq 13$ ;  $0 \leq k \leq 6$ ;  $0 \leq l \leq 17$ ) using  $\theta$ - $2\theta$  scans. Three standard reflections measured every 6000 s of exposure showed no loss of intensity ( $\pm 1\%$ ). 1105 reflections were measured, with 898 unique and 791 observed [ $I > 2\sigma(I)$ ]. Merging  $R$ -value on intensities was 0.008. The function minimized during refinement was  $\sum w(|F_o| - |F_c|)^2$  with  $w = 1/[(\sigma F_o)^2 + (0.001 \cdot F_o^2)]$ . All H atom positions were found from difference Fourier maps, and the  $xyz$  positional parameters were refined with fixed isotropic temperature factors at 1.3-times that of the atom attached. All other atoms were refined with anisotropic temperature factors. An isotropic extinction coefficient was refined and found to be insignificant. 103 parameters were refined in the final least-squares analysis which gave  $R = 0.030$ ,  $R_w = 0.032$ , and  $S = 2.52$ . The  $(\Delta/\sigma)_{\text{max}}$  in the final cycle was 0.001. The final difference map electron density maximum was 0.71 and the minimum was  $-0.27\text{ e}/\text{\AA}^3$ . Atomic scattering factors were taken from *The International Tables for X-ray Crystallography*.<sup>23</sup> Least-squares refinement on  $F_o$  was performed using the NRCVAX suite of programs.<sup>24</sup>

**Theoretical Methods.** In the choice of the best compromise between accuracy and computational demand, we selected theoretical levels that match or exceed the quality reached by Sengupta and Chandra,<sup>13</sup> Lin et al.,<sup>14</sup> and Shancke

et al.<sup>21</sup> Our choice of theoretical model reflects the fact that the computation of correlation corrections to energies is more sensitive to the choice of the theoretical model than to the structural changes. Potential energy hypersurface analysis included a perturbational treatment of electron correlation using second-order Møller–Plesset theory.<sup>25,26</sup> Restricted Hartree–Fock (RHF) reference wave functions were employed for all molecules with the exception of the calculations of the triplet states of RNO (and of  $\text{C}_2\text{O}_2$ ) which employed unrestricted Hartree–Fock (UHF) reference wave functions. The structural effects of spin contamination of the UHF solutions are minimal since the annihilation operator commutes with the charge density operator.<sup>27</sup> The 6-31G\* basis set was used and this theoretical level is thus denoted MP2(full)/6-31G\*. All molecules were optimized under the constraints imposed by the symmetry point groups specified. Analytical first and second derivatives were then computed for each structure at the same theoretical level to confirm that the structure is indeed stationary on the potential energy hypersurface, to determine whether a minimum or a transition state structure had been located via the number of imaginary frequencies (NIMAG), and to obtain vibrational zero-point energies (VZPE) and all other thermodynamical functions. The vibrational properties computed at this correlated level are reported as calculated and without scaling.<sup>28</sup> Assignments of the normal modes were made visually with the program Vibrate.<sup>29</sup> More reliable energies were determined using full fourth-order Møller–Plesset perturbation theory,<sup>30</sup> MP4(sdtq), as well as quadratic configuration interaction theory<sup>31</sup> that included single and double excitations and also corrections for triplet excitation, QCISD(T). The higher level calculations employed the fully polarized valence triple- $\zeta$  quality basis set 6-311G\*\*. The frozen core approximation was used in the higher-level MPx and QCISD(T) calculations. The best theoretical model employed is represented by the notation QCISD(T)/6-311G\*\*/MP2(fu)/6-31G\* +  $\Delta\text{VZPE}(\text{MP2}/6-31\text{G}^*)$ . For the dimers **5**, the highest theoretical level differed in that the higher level correlated energies were computed with the 6-31G\* basis set. Calculations were carried out with Gaussian92/DFT<sup>32</sup> on SGI Indigo and IBM RS-6000 systems, and the results of the potential energy surface analysis are summarized in Tables 5 and 6 and pertinent thermochemical data are summarized in Table 7. In Tables 5 and 6, basis sets A and B refer to 6-31G\* and 6-311G\*\*, respectively, and these basis sets were used with six and five d-functions, respectively. The data in Tables 5 and 6 show just how critical it is to employ ab initio methods that account well for electron correlation effects. We included the HF energies obtained at the HF/B//MP2/A level, and Table 6 shows that especially the binding energies  $E_b$  and the singlet–triplet gaps  $E_{1-3}$  require higher correlated levels. Note that the  $E_{1-3}$  values have the wrong sign at the HF level. We also determined the energies of the  $^3A''$  states at the PUGH, PMP2, and PMP3 levels, that is, after annihilation of the spin contaminants due to the spin states  $s + 1$  through  $s + 3$  via spin projection techniques. The respective total energies are listed at the bottom of Table 5 and the  $E_{1-3}$  values after spin projection are given in Table 6 below the respective value

(25) Hehre, W. J.; Radom, L.; Schleyer, P. v. R.; Pople, J. A. *Ab Initio Molecular Orbital Theory*; Wiley & Sons: New York, 1986.

(26) Pople, J. A.; Krishnan, R.; Schlegel, H. B.; Binkley, J. S. *Int. J. Quant. Chem.* **1978**, *14*, 91.

(27) Glaser, R.; Choy, G. S.-C. *J. Phys. Chem.* **1993**, *97*, 3188, and references cited there.

(28) Hout, R. F.; Levi, B. A.; Hehre, W. J. *J. Comput. Chem.* **1982**, *3*, 234.

(29) Vibrate 2.0: Glaser, R.; Chladny, B. S.; Hall, M. K. *Quantum Chemistry Program Exchange, QCPE Bulletin* **1993**, *13*, 75.

(30) (a) Krishnan, R.; Pople, J. A. *Int. J. Quant. Chem.* **1978**, *14*, 91. (b) Krishnan, R.; Frisch, M. J.; Pople, J. A. *J. Chem. Phys.* **1980**, *72*, 4244.

(31) Pople, J. A.; Head-Gordon, M.; Raghavachari, K. *J. Chem. Phys.* **1987**, *87*, 5968.

(32) Gaussian 92/DFT, Revision G.2, M. J. Frisch, G. W. Trucks, H. B. Schlegel, P. M. W. Gill, B. G. Johnson, M. W. Wong, J. B. Foresman, M. A. Robb, M. Head-Gordon, E. S. Replogle, R. Gomperts, J. L. Andres, K. Raghavachari, J. S. Binkley, C. Gonzalez, R. L. Martin, D. J. Fox, D. J. Defrees, J. Baker, J. J. P. Stewart, and J. A. Pople, Gaussian, Inc., Pittsburgh, PA, 1993, and references cited there.

(22) For a pertinent recent discussion, see: Glaser, R.; Chen, G. S.; Anthamatten, M.; Barnes, C. L. *J. Chem. Soc., Perkin Trans. 2* **1995**, 1449.

(23) *International Tables for X-Ray Crystallography*; Kynoch Press, Birmingham (Present distributor: Kluwer Academic Publishers, Dordrecht); Vol. IV.

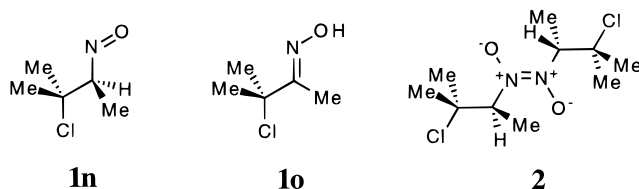
(24) Frenz, B. A. Enraf-Nonius Structure Determination Package. Enraf-Nonius Delft, The Netherlands, 1985.

calculated *without* spin projection to allow for an appreciation of the magnitude of energetic effects of electron correlation and/or spin contamination. Electronic structures are described by *molecular* and *atomic* parameters evaluated with MP2(full)/6-31G\* wave functions. As molecular properties, we report the dipole and quadrupole moments. The natural bond orbital method (NBO) was employed to determine atom populations.<sup>33</sup>

## Results and Discussion

**Preparation, Structural Studies in Solution, and X-ray Structure of the *Trans*-Dimer of 2-Chloro-2-methyl-3-nitrosobutane.** It has long been known that  $\alpha$ -nitroso halides can be prepared by addition of nitrosyl halides NOX (X = Cl, Br, NO<sub>2</sub>) to olefins.<sup>17</sup> The reaction has been studied mechanistically,<sup>34</sup> and it is widely utilized.<sup>35</sup> *In situ* preparation of the reagent from alkyl nitrite and acid avoids handling noxious NOX while maintaining reasonable yields.<sup>36</sup> However, in the majority of cases the yields of crystalline product are only in the range of 40–50%. In particular, electron-withdrawing groups on the olefin<sup>37</sup> often prevent reaction altogether and steric effects can also be important. The nitroso chloride of 2-methyl-2-butene was prepared by reaction with NOCl(g), and *in situ* formation of NOCl (isoamyl nitrite and concd HCl) also was employed. The expected addition regiochemistry was found and yields of about 40% were realized. The colorless product had a melting point of 75–6 °C after crystallization from methanol.

Several structures have to be considered for the “nitroso chloride of 2-methyl-2-butene” and they include the monomers **1n** and **1o** and the bis(1,2-dimethyl-2-chloropropyl)diazene dioxide **2**. In general, the products of NOCl addition to olefins are colorless and dimeric in solution and in the solid state. Dissociation into bluish diamagnetic monomers usually occurs when the dimers



are dissolved and/or heated in an inert, low polarity solvent (i.e. CH<sub>2</sub>Cl<sub>2</sub> or ether) and the monomers revert to the dimer at a rate thought to be slow<sup>37</sup> or fast<sup>38</sup> depending on solvent and other conditions. The dimer formation often is established by molecular weight (MW) determinations based on melting point depression measurements and assumed to involve NN connection between two nitroso compounds. However, the nitroso compounds often tautomerize during or after preparation to oximes which may have considerable thermodynamic and kinetic stability. In fact, Thorne claimed that refluxing 2-chloro-2-methyl-3-nitrosobutane in alcohol

(33) NBO review: Weinhold, F.; Carpenter, J. E. In *The Structure of Small Molecules and Ions*; Naaman, R., Vager, Z., Eds.; Plenum Press: New York, 1988; p 227ff.

(34) Meinwald, J.; Meinwald, Y. C.; Baker, T. N., III. *J. Am. Chem. Soc.* **1964**, *86*, 4074.

(35) Beckham, L. J.; Fessler, W. A.; Kise, M. A. *Chem. Rev.* **1951**, *48*, 319.

(36) (a) Hickinbottom, W. J. *Reactions of Organic Compounds*; Longmans, Green & Co.: New York, 1936; pp 20–23. (b) Wallach, O. *Chem. Ber.* **1895**, *28*, 1308.

(37) Thorne, N. *J. Chem. Soc.* **1956**, 2587, 4271.

(38) (a) March, J. *Advanced Organic Chemistry*, 3rd ed.; Wiley & Sons: New York, 1985; p 729. (b) *Ibid.* p 18.

**Table 1. Positional Parameters and Their Estimated Standard Deviations of the *trans*-Dimer of 2-Chloro-2-methyl-3-nitrosobutane<sup>a</sup>**

atom	x	y	z	B <sub>iso</sub>
Cl	0.56363(4)	0.22151(9)	0.24668(3)	2.30(3) <sup>c</sup>
O	0.53739(15)	0.20678(25)	0.54721(9)	2.54(8)
N	0.50764(16)	0.08913(28)	0.49094(11)	1.46(8)
C1	0.67850(20)	0.02746(47)	0.36654(16)	1.77(11)
C2	0.59823(18)	0.19805(37)	0.35906(13)	1.66(10)
C3	0.48453(18)	0.15343(37)	0.40183(13)	1.48(10)
C4	0.40333(21)	0.31549(42)	0.40553(16)	2.07(11)
C5	0.65145(22)	0.37982(45)	0.38706(17)	2.38(12)
HC3	0.4541(21)	0.0467(38)	0.3763(14)	2.2 <sup>b</sup>
H1C1	0.6486(24)	−0.0686(44)	0.3573(16)	2.5
H2C1	0.7242(24)	0.0445(43)	0.3413(16)	2.5
H3C1	0.6984(21)	0.0287(42)	0.4147(16)	2.5
H1C4	0.3849(21)	0.3575(42)	0.3533(16)	2.8
H2C4	0.4341(22)	0.4230(40)	0.4386(15)	2.8
H3C4	0.3373(22)	0.2782(38)	0.4321(14)	2.8
H1C5	0.7135(25)	0.3981(41)	0.3607(16)	3.2
H2C5	0.6653(22)	0.3745(41)	0.4444(15)	3.2
H3C5	0.6027(23)	0.4980(46)	0.3790(15)	3.2

<sup>a</sup> Numbers in parentheses are estimated standard deviations in the least significant figures. <sup>b</sup> Hydrogens have fixed isotropic temperature factors 1.3 times that of the attached atom. <sup>c</sup> B<sub>iso</sub> is the mean of the principal axes of the thermal ellipsoid.

**Table 2. Bond Distances (Å) and Bond and Dihedral Angles (deg) of the *trans*-Dimer of 2-Chloro-2-methyl-3-nitrosobutane**

parameter	value <sup>a</sup>	parameter	value <sup>a</sup>
Cl–C2	1.823(2)	C1–C2	1.555(4)
O–N	1.270(3)	C2–C3	1.554(3)
N–N <sub>a</sub>	1.315(4)	C2–C5	1.509(4)
N–C3	1.500(3)	C3–C4	1.512(4)
O–N–N <sub>a</sub>	121.75(19)	C1–C2–C3	110.49(21)
O–N–C3	120.02(19)	C1–C2–C5	112.88(21)
N <sub>a</sub> –N–C3	118.19(19)	C3–C2–C5	114.79(20)
Cl–C2–C1	106.49(16)	N–C3–C2	107.94(17)
Cl–C2–C3	104.02(15)	N–C3–C4	108.32(19)
Cl–C2–C5	107.39(18)	C2–C3–C4	115.18(21)
O–N–C3–C2	73.7(2)	O–N–C3–C4	−51.7(2)
C1–C2–C3–N	167.4(2)	C1–C2–C3–C4	−71.4(2)
C2–C2–C3–N	53.4(2)	C1–C2–C3–C4	174.7(3)
C5–C2–C3–N	−75.5(2)	C5–C2–C3–C4	45.6(2)

<sup>a</sup> Numbers in parentheses are estimated standard deviations in the least significant digits. <sup>b</sup> N<sub>a</sub> is the symmetry equivalent of N at 1 – x, –y, 1 – z.

produces a yellow solution of 2-chloro-2-methylbutan-3-one oxime in high yield and without appreciable chlorine substitution. Hence, it was desirable to ascertain the structure of the prepared material in the solid state and in solution. Saturated methanol solutions of the addition product were prepared at room temperature, and single crystals suitable for X-ray structural studies were obtained by slowly cooling the solutions and by solvent evaporation in a freezer at –5 °C. The structure was solved (*vide supra*) and found to contain an inversion-symmetric NN-connected *trans*-dimer **2** of 2-chloro-2-methyl-3-nitrosobutane. Final positional parameters are given in Table 1, major structural parameters are contained in Table 2, and information regarding the calculated least-square plane formed by O,O',N,N',C3-,C3' is given in Table 3. Within experimental error (0.02 Å) all heavy atoms lie within a single plane. The molecule is not involved in any significant intra- or intermolecular hydrogen bonding.<sup>39</sup> The sharpness of the dif-

(39) The closest intermolecular approach to hydrogen are approaches of N to HC3 (1.937(10), 2.347(12)) and of O to HC3 (2.174(15) Å), and both of these are too far removed to be of structural importance.

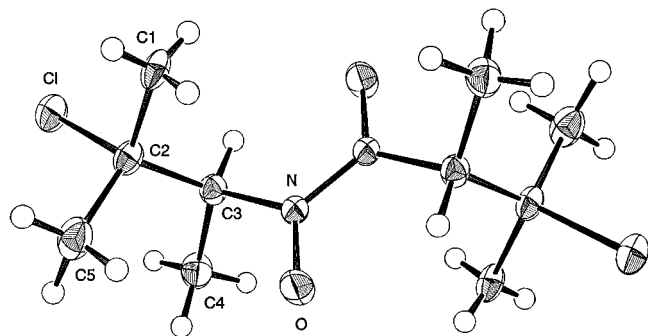


**Figure 1.** ORTEP drawing of the *trans*-dimer of 2-chloro-2-methyl-3-nitrosobutane, **2**, with numbering scheme.

**Table 3.** Deviations from Best Molecular Plane (O,N,C3,O',N',C3')

equation of the plane: $11.447X - 1.208Y - 3.864Z - 3.795 = 0$		
Distances of Atoms from the Plane		
O: -0.007	N: 0.012	C3: 0.014
Distances to Other Atoms		
C1: 1.436	C1': 2.522	C4: -1.126
C2: 1.420	C5: 1.708	HC3: -0.11

<sup>a</sup> The primed atoms are symmetry related by  $1 - x, -y, 1 - z$ .

**Table 4.** <sup>1</sup>H- and <sup>13</sup>C-NMR Spectroscopy<sup>a</sup>

	<sup>13</sup> C-NMR $\delta$ (ppm)	$\delta$ (ppm)	<sup>1</sup> H-NMR <sup>b</sup> integr	mult
C1	29.26	1.65	3	s
C2	69.32			
C3	66.92	5.96	1	q, 6.8 Hz
C4	13.54	1.49	3	q, 6.8 Hz
C5	28.99	1.68	3	

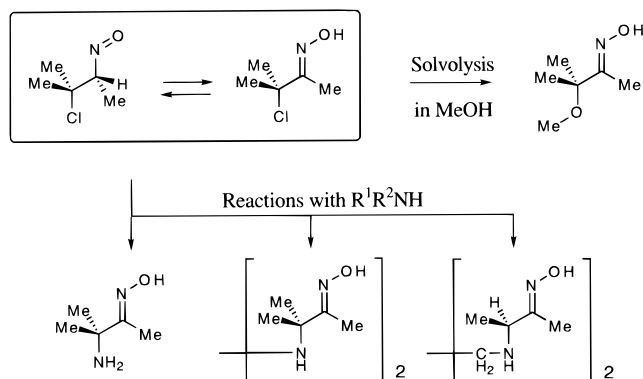
<sup>a</sup> CDCl<sub>3</sub>, 500 MHz, 23 °C, TMS standard. <sup>b</sup> Chemical shifts  $\delta$  (ppm) of <sup>1</sup>H NMR of impurity (4%): 5.95 (q), 1.72, 1.70, 1.48 (d).

fraction peaks as well as the low temperature factors suggest well ordered crystals with small thermal motion of the atoms. Consequently, the H atom positions could be well defined.

An ORTEP drawing of **2** is shown in Figure 1. The conformations about the C3–N bonds are such as to eclipse the C3–H bonds with the N=N bond presumably to optimize electrostatic attraction between the H-atoms at C3 and the proximate O-atoms. Staggered conformations about the C2–C3 bonds are realized that place the largest substituents in *s-trans* arrangements. The diazene dioxide nature of the dimer—rather than a dimeric oxime structure—is clearly evidenced by the short N–O and long C–N distances. The sp<sup>3</sup>–sp<sup>3</sup> C–C distances average 1.533 Å and are typical. The C–Cl distance of 1.823(4) Å is slightly longer than the usual value of 1.78 Å. C–N single bonds in amines are close to 1.47 Å, and the C3–N bond in the diazene dioxide is slightly elongated to 1.500(3) Å. The N–O bond distance is 1.270(3) Å and the N–N bond length of 1.315(4) Å is much shorter than a single bond and more like a double bond (1.27 Å). Both bond lengths are in the typical ranges for diazene dioxides.

The <sup>1</sup>H and <sup>13</sup>C NMR results are summarized in Table 4. The signal at  $\delta = 66.92$  ppm was assigned to C3 (as opposed to C2) using a DEPT90 experiment. The relative intensities and splitting patterns of the <sup>1</sup>H resonances indicate a symmetric structure and agree with the diazene dioxide structure. The NMR spectra showed a second set of weak peaks somewhat displaced from the main signals. These signals are assigned to the mono-

**Scheme 1**



meric nitroso compound **1n**, and its concentration was estimated to be less than 4%. Examination of solutions 15 and 30 min (22 °C) after dissolution in CDCl<sub>3</sub> (with TMS) showed no change in the intensity of these peaks. Since warming of diazene dioxides in solvents of low polarity is known to cause dissociation into nitroso compounds (*vide supra*), our results suggest that the dissociation rate is slow at room temperature and that the small amount of monomer present was *not* formed by dissociation but rather might have been introduced into the solution as impurity absorbed on the surface of the crystalline sample. Refluxing the diazene dioxide in ethanol does not give the monomer cleanly and precluded a definitive answer to the question as to whether the monomer prefers the oxime or nitroso structure. Nevertheless, circumstantial evidence indicates that both isomers are present at least in small amounts. Refluxing of **2** in ethanol and subsequent solvent removal resulted in white crystals (15%) and oil. The crystals were identified as hydroxylamine hydrochloride based on their X-ray unit cell dimensions. The oil did not crystallize even after a long period at low temperature. The identification of H<sub>2</sub>NOH·HCl suggests that hydrolysis of oxime **1o** occurred. We showed previously that several closely related compounds in which chlorine is replaced by an amino or hydrazino group do in fact crystallize as oximes<sup>40</sup> (Scheme 1). Furthermore, solvolysis of the nitroso chloride in alcohols leads to nucleophilic replacement of chlorine, the resulting methyl ether derivative of **1o** was isolated in a rhodium(III) complex, and the X-ray structure showed the oxime tautomer.<sup>41</sup>

**Conformational and Configurational Preferences in Diazene Dioxides.** The *C*<sub>2h</sub> and *C*<sub>2v</sub> symmetric *trans*- and *cis*-*N,N*-dioxodiazenes **3**, respectively, are shown in Figure 2, and the structural parameters of monomeric HNO are given in italics. The *trans* preference energy shows only a modest dependency on the theoretical level of calculation and at our highest level we found a value of *E*<sub>c-t</sub> = 4.0 kcal/mol (Table 6). For the mixed dimer **4** (Figure 3), we considered two structures with the same NN *trans* arrangement but with different N–C conformations. We will characterize conformations by the dihedral angle  $\tau = \angle(\text{O–N–C–H})$ . The structure with dihedral angle  $\tau = 0^\circ$  is found to be the minimum (left in Figure

(40) (a) Structure of 3,3'-(ethylenediimino)bis(3-methyl-2-butanone oxime), C<sub>12</sub>H<sub>26</sub>N<sub>4</sub>O<sub>2</sub>; Hussein, M. S.; Hague, M. *Acta Crystallogr.* **1983**, *C39*, 292. (b) Structure of bis(2-methyl-3-butanone oxime)hydrazine; Murmann, R. K.; Schlemper, E. O.; Barnes, C. L. *J. Crystallogr. Spectrosc. Res.* **1993**, *23*, 675. (c) Crystal structure of 3-methyl-3-amino-2-butanone oxime (P21, *a* = 9.225, *b* = 10.937, *c* = 6.943,  $\beta$  = 106.5, *V* = 671.7, *R* = 0.04, *R*<sub>w</sub> = 0.048); Murmann, R. K., to be published.

(41) Efñ, G. E.; Schlemper, E. O. *Polyhedron* **1991**, *10*, 1611.

**Table 5. Total Energies and Vibrational Zero-Point Energies**

property <sup>a-c</sup>	HNO, <sup>1</sup> A' C <sub>s</sub>	HNO, <sup>3</sup> A'' C <sub>s</sub>	<i>trans</i> - <b>3</b> C <sub>2h</sub>	<i>cis</i> - <b>3</b> C <sub>2v</sub>	H <sub>2</sub> C=NOH C <sub>s</sub>
E(MP2/A)	-130.130164	-130.095434	-260.302266	-260.29626	-169.320810
VZPE(MP2/A)	8.70	9.71	23.89	23.42	28.2
NIMAG(MP2/A)	0	0	0	0	0
HF/B//MP2/A	-129.815369	-129.822413	-259.619771	-259.610217	-168.888120
MP2/B//MP2/A	-130.193195	-130.159693	-260.425832	-260.421457	-169.409794
MP3/B//MP2/A	-130.190565	-130.164230	-260.395202	-260.389501	-169.420789
MP4sdtq/B//MP2/A	-130.219442	-130.185308	-260.472231	-260.465567	-169.451766
QCISD(T)/B//MP2/A	-130.216935	-130.186220	-260.456941	-260.449853	-169.451319
property	MeNO, <sup>1</sup> A' C <sub>s</sub> , τ = 180°	MeNO, <sup>3</sup> A'' C <sub>s</sub> , τ = 180°	MeNO, <sup>1</sup> A' C <sub>s</sub> , τ = 0°	MeNO, <sup>1</sup> A' C <sub>s</sub> , τ = 0°	MeNO, <sup>3</sup> A'' C <sub>s</sub> , τ = 0°
E(MP2/A)	-169.306316	-169.269560	-169.308084		-169.267823
VZPE(MP2/A)	27.55	29.01	27.72		28.74
NIMAG(MP2/A)	1	0	0		1
HF/B//MP2/A	-168.865162	-168.869088	-168.867444	-168.823121 <sup>b</sup>	-168.866030
MP2/B//MP2/A	-169.390678	-169.353625	-169.392439	-169.297687 <sup>b</sup>	-169.351676
MP3/B//MP2/A	-169.397749	-169.368611	-169.399628	-169.306208 <sup>b</sup>	-169.366245
MP4sdtq/B//MP2/A	-169.435761	-169.398165	-169.437240	-169.337417 <sup>b</sup>	-169.395999
QCISD(T)/B//MP2/A	-169.432806	-169.398970	-169.434344	-169.335842 <sup>b</sup>	-169.396426
property	<i>trans</i> - <b>4</b> C <sub>s</sub> , τ = 180°	<i>trans</i> - <b>4</b> C <sub>s</sub> , τ = 0°	<i>cis</i> - <b>5</b> C <sub>2v</sub> , τ = 0°	<i>cis</i> - <b>5</b> C <sub>2</sub>	<i>trans</i> - <b>5</b> C <sub>2h</sub> , τ = 0°
E(MP2/A)	-299.481293	-299.482340	-338.641699	-338.642146	-338.661250
VZPE(MP2/A)	42.16	42.33	60.08	60.47	60.60
NIMAG(MP2/A)	1	0	1	0	0
HF/B//MP2/A	-298.671492	-298.673749		-337.606498 <sup>b</sup>	-337.634517 <sup>b</sup>
MP2/B//MP2/A	-299.625357	-299.626377		-338.620243 <sup>b</sup>	-338.639227 <sup>b</sup>
MP3/B//MP2/A	-299.604212	-299.606113		-338.608880 <sup>b</sup>	-338.631028 <sup>b</sup>
MP4sdtq/B//MP2/A	-299.689480	-299.690143		-338.689133 <sup>b</sup>	-338.709111 <sup>b</sup>
QCISD(T)/B//MP2/A	-299.673946	-299.675152		-338.675604 <sup>b</sup>	-338.696841 <sup>b</sup>
property <sup>d</sup>	HNO, <sup>3</sup> A'' C <sub>s</sub>	MeNO, <sup>3</sup> A'' C <sub>s</sub> , τ = 180°	MeNO, <sup>3</sup> A'' C <sub>s</sub> , τ = 0°		
PUHF/B//MP2/A	-129.830229	-168.876912	-168.873913		
PMP2/B//MP2/A	-130.164304	-169.358299	-169.356380		
PMP3/B//MP2/A	-130.166322	-169.370781	-169.368416		

<sup>a</sup> Basis sets A and B are 6-31G\* and 6-311G\*\*, respectively. <sup>b</sup> For the nitrosomethane dimers, the higher level energies were computed with basis sets A and B being 6-31G\*. <sup>c</sup> Total energies in atomic units and vibrational zero-point energies in kcal/mol. <sup>d</sup> Energies at the PUHF, PMP2, and PMP3 levels determined after annihilation of quintet, septet, and nonet states via spin projection.

**Table 6. Isomer Preferences, Rotational Barriers, Excitation Energies, Tautomerization Energies, and Dimer Formation Energies**

energy parameter <sup>a,b</sup>	ΔVZPE	MP2/A	HF/B <sup>c</sup>	MP2/B	MP3/B	MP4sdtq/B	QCISD(T)/B
Singlet-Triplet Gap, $E_{1-3}$							
HNO, <sup>3</sup> A'' vs <sup>1</sup> A'	1.01	21.79	-4.42	21.02	16.53	21.42	19.27
MeNO, <sup>3</sup> A'', τ = 180° vs <sup>1</sup> A', τ = 0°	1.29	24.17	-1.03	24.36	19.46	24.52	22.20
MeNO, <sup>3</sup> A'', τ = 0° vs <sup>1</sup> A', τ = 0°	-0.17	25.26	0.89	22.58	20.95	25.88	23.79
Isomer Preference Energies, $E_{c-t}$							
<b>3</b> , <i>cis</i> vs <i>trans</i>	-0.47	3.77	6.00	2.75	3.58	4.18	4.43
<b>5</b> , <i>cis</i> -C <sub>2</sub> vs <i>trans</i> -C <sub>2h</sub>	-0.13	11.99	17.58	11.91	13.90	12.54	13.33
Barriers to Interconversion, $E_{rot}$ or $E_{enant}$							
MeNO, <sup>1</sup> A', $E_{rot}$ , τ = 180° vs τ = 0°	-0.17	1.11	1.43	1.11	1.18	0.93	0.97
MeNO, <sup>3</sup> A'', $E_{rot}$ , τ = 0° vs τ = 180°	-0.27	1.09	1.92	1.22	1.48	1.36	1.60
<i>trans</i> - <b>4</b> , C <sub>s</sub> , $E_{rot}$ , τ = 180° vs τ = 0°	-0.17	0.66	1.42	0.64	1.19	0.42	0.76
<i>cis</i> - <b>5</b> , C <sub>2v</sub> vs C <sub>2</sub> , $E_{enant}$	-0.39 <sup>d</sup>	0.28					
Oxime-Nitroso Tautomerization Energy, $E_{taut}$							
MeNO ( <sup>1</sup> A', τ = 0°) vs H <sub>2</sub> C=NOH	0.48	7.99	12.97	10.89	13.28	9.12	10.65
Dimer Formation Energies, $E_d = -E_b$							
<i>trans</i> - <b>3</b>	6.49	-26.32	6.88	-24.75	-8.83	-20.93	-14.46
<i>trans</i> - <b>4</b> (τ = 0°)	5.91	-27.67	5.69	-25.57	-9.99	-21.00	-14.98
<i>trans</i> - <b>5</b>	5.16	-28.29	7.36	-27.52	-11.68	-21.51	-15.79

<sup>a</sup> All data in kcal/mol and based on MP2(full)/6-31G\* structures. All dimer formation energies are relative to the ground states of HNO and MeNO (τ = 0°). <sup>b</sup> For **5**, the higher level energies were computed with basis sets A and B being 6-31G\*. <sup>c</sup> RHF and UHF for closed- and open-shell systems computed at HF/B//MP2/A.  $E_{1-3}$  values given in italics are based on PUHF, PMP2, and PMP3 energies of the triplet state. <sup>d</sup> See text.

3) while the other structure is the transition state structure for methyl rotation. Our best estimate for this rotational barrier is  $E_{rot} = 0.6$  kcal/mol. Note that this

conformational preference carries over from MeNO itself for which the rotation about the C-N bond is essentially unhindered ( $E_{rot} = 0.8$  kcal/mol). The *cis* and *trans*

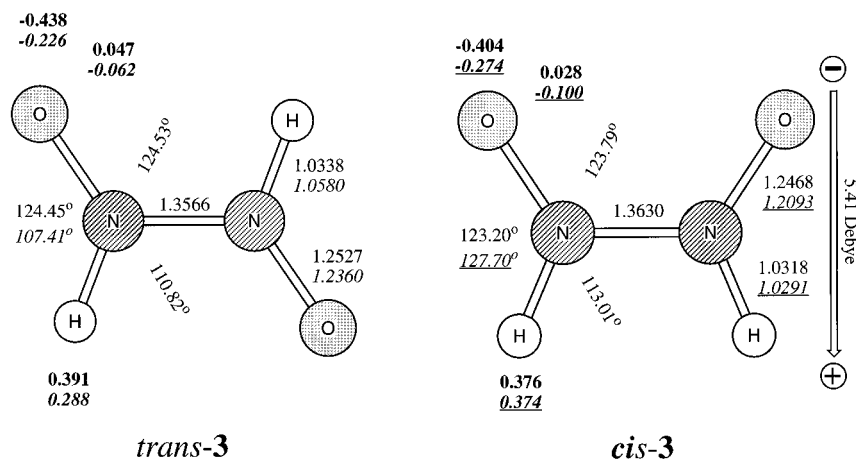


**Figure 2.** MP2(full)/6-31G\* optimized structures of the planar *trans* ( $C_{2h}$ ) and *cis* ( $C_{2v}$ ) HNO dimers, **3**. The NBO atomic charges determined with the MP2(full)/6-31G\* wave function are given in bold. Values in italics always refer to the respective monomer. Underlined data refer to the first triplet state of HNO.

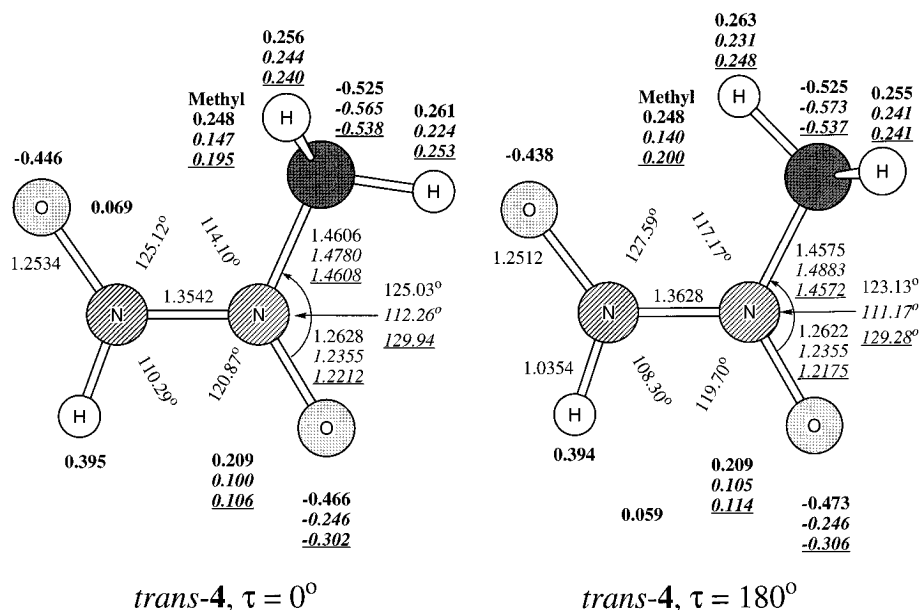


**Figure 3.** MP2(full)/6-31G\* optimized structures of the two conformations examined for the  $C_s$  symmetric *trans* dimers **4** derived from HNO and MeNO. The MP2(full)/6-31G\* NBO atomic charges are given in bold. Values in italics refer to the monomer MeNO in the conformation shown and underlined data again refer to the respective triplet state.

isomers of nitrosomethane dimer **5** are shown in Figure 4. In contrast to the earlier RHF/4-31G level study by Minato et al.,<sup>20</sup> the  $C_{2v}$  symmetric structure of *cis-5* does not correspond to a minimum but rather represents a transition state structure ( $a_2$ ,  $1141 \text{ cm}^{-1}$ ) for enantiomerization between the  $C_2$  symmetric minima. Aside from the orientation of the methyl groups, the  $C_{2v}$  and the  $C_2$  structures differ in that the  $C_2$  structure shows a modest tendency toward N-pyramidalization as is illustrated by the side-on view in Figure 4. These characteristic features also have been found in the solid state structures of the *cis* dimers formed by azobenzene dioxide and its perfluoro derivative.<sup>5</sup> While packing effects might have been responsible for the observed  $C_2$  symmetry in the solid state, the calculational results suggest that the  $C_2$  symmetry is *intrinsically* preferred. The energetic consequences of all these distortions are minor; the enantiomerization requires less than 1 kcal/mol at the level of optimization.<sup>42</sup> The  $C_{2h}$ -symmetric *trans-5* is thermodynamically greatly preferred. At the highest level of

calculation, a *trans* preference energy of  $E_{c-t} = 13.2 \text{ kcal/mol}$  is predicted.

The computed structures of HNO and of MeNO can be compared to experimental data. From the rotational fine-structure of the vibrational absorption spectrum of HNO, Dalby<sup>43</sup> determined the structure of the ground state of HNO ( $\text{NO} = 1.211_6 \text{ \AA}$ ,  $\text{NH} = 1.062_8 \text{ \AA}$ ,  $\angle(\text{H}-\text{N}-\text{O}) = 108.5_8^\circ$ ), and the agreement between theory and

(42) A noteworthy technicality relates to the VZPE corrections to the relative stabilities of the  $C_{2v}$  and  $C_2$  structures. The structures, force constants, and frequencies are very similar. Yet, for the  $C_2$  structure, the lowest frequency is positive and included in VZPE while the lowest frequency for  $C_{2v}$  structure is imaginary and omitted. The VZPE term is thus greater for the  $C_2$  structure, and the calculated difference is so large as to indicate a reversal of the relative stability of the  $C_{2v}$  and  $C_2$  structures if the  $\Delta\text{VZPE}$  term were considered. This conclusion cannot be drawn, however, since the lowest frequencies also are the least accurate and because  $\Delta\text{VZPE}$  is dominated by the term  $h[\nu_1^{\text{imag}}(C_{2v}) - \nu_1(C_2)]$  since the terms  $h[\nu_1(C_{2v}) - \nu_1(C_2)]$  are small for all other respective frequencies.

(43) (a) Dalby, F. W. *Can. J. Phys.* **1958**, *36*, 1336. (b) Herzberg, G. *Electronic Spectra of Polyatomic Molecules*; Nostrand Reinhold Co.: New York, 1966; p 589.

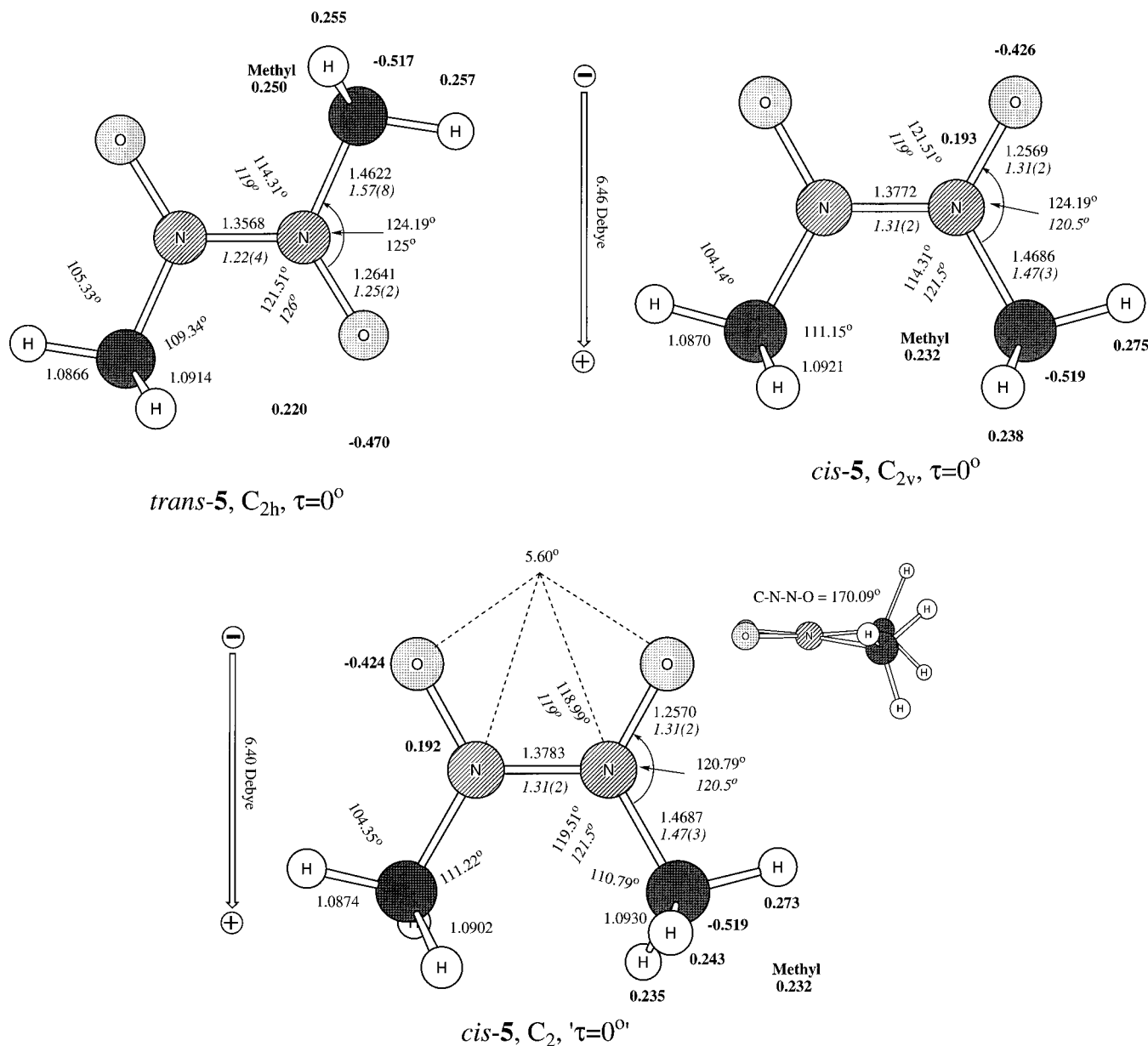


**Figure 4.** MP2(full)/6-31G\* optimized structures of *trans* and *cis* nitrosomethane dimers, **5**. The MP2(full)/6-31G\* NBO atomic charges are given in bold. Values in italics refer to the solid state data determined by X-ray crystallography.

experiment is very good. The two high-frequency vibrations computed for HNO are overestimated somewhat (by 5.4 and 12.0%) at the MP2 level compared to experiment<sup>43</sup> ( $\nu_1 = 2854.2$ ;  $\nu_2 = 1420.8$ ;  $\nu_3 = 981.2$ ) while the predicted frequency  $\nu_3$  is much too high. In 1978, Turner and Cox<sup>44</sup> measured the microwave spectra of isotopomers of MeNO. A conformational preference for the  $\tau = 0^\circ$  structure was found, and the agreement of major structural parameters (NO = 1.211 Å, CN = 1.480 Å,  $\angle(\text{O-N-C}) = 113.2^\circ$ ) is very good. Importantly, the measured dipole moment of 2.320(4) Debye is in excellent agreement with the theoretical value obtained with the MP2(full)/6-31G\* level while the reported HF/4-31G value of 3.12 Debye<sup>20</sup> greatly overestimates the polarity. Much less experimental data exist for the dimers. Christie, Frost, and Voisey<sup>45</sup> showed that *trans-5* is preferred at room temperature, and their observation is

in agreement with theory. Meerssche et al. succeeded at the determination of the solid state structures of both isomers of **5**, and these experimental data are included in Figure 4. Neither of these X-ray structure determinations were well refined by today's standards, and the major significance of these reports lies more with providing proof for the existence of both isomers rather than with the precise structural parameter measurements. The theoretical NO bond lengths (1.251–1.264 Å) compare very well to the values in other diazene dioxides whose structures were determined more accurately, and the predicted NN bond lengths (1.354–1.379 Å) are slightly longer but the agreement is still quite good.<sup>46</sup>

**Thermochemistry of the Diazene Dioxide Formation.** The reaction enthalpy at room temperature,  $\Delta H(298)$ , considers volume work in addition to changes in internal energy differences. The volume work  $\Delta(PV)$  equals  $-RT$  ( $-0.59$  kcal/mol) since dimer formation re-

(44) MW structure and dipole moment of MeNO: Turner, P. H.; Cox, A. P. *J. Chem. Soc., Faraday Trans. 2* **1978**, *74*, 533.

(45) Christie, M. I.; Frost, J. S.; Voisey, M. A. *Trans. Faraday Soc.* **1965**, *61*, 674.

(46) See, for example, Table V in the paper by Dietrich, Paul, and Curtin (ref 4e).



**Table 7. Thermochemistry of Diazene Dioxide Formations**

property	HNO	MeNO, $\tau = 0^\circ$	<i>trans</i> - <b>3</b>	<i>trans</i> - <b>4</b>	<i>trans</i> - <b>5</b>
VZPE	8.70	27.72	23.89	42.33	60.60
$\Delta E_{\text{vib}}(298)$	0.01	0.60	0.77	1.57	4.21
$E_{\text{rot}}(298)$	0.89	0.89	0.89	0.89	0.89
$E_{\text{trans}}(298)$	0.89	0.89	0.89	0.89	0.89
$E_{\text{total}}(298)$	10.49	30.10	26.44	45.67	66.59
$S_{\text{trans}}$	36.23	37.34	38.29	38.90	39.41
$S_{\text{rot}}$	16.58	21.37	21.61	25.21	24.97
$S_{\text{vib}}$	0.02	3.55	3.81	8.67	13.76
$S(298)$	52.83	62.26	63.71	72.78	78.13
$\Delta E_{\text{elect}} = -E_{\text{b}}$			-14.46	-14.98	-15.79
$\Delta \text{VZPE}$			6.49	5.91	5.16
$-E_{\text{b}}^{\text{corr}}$			-7.97	-9.07	-10.63
$\Delta E(298)$			-9.00	-9.89	-9.40
$\Delta H(298)$			-9.59	-10.48	-9.99
$\Delta S(298)$			-41.95	-42.31	-46.39

<sup>a</sup> All data in kcal/mol except for entropy data which are in cal/mol K.  $\Delta E_{\text{elect}}$  from highest level data (preceding table).

duces the number of moles by one. The term  $\Delta E(298)$  contains the energy difference  $\Delta E_{\text{elect}}$  between the diazene

$$\Delta H(298) = \Delta E(298) + \Delta(PV)$$

$$\Delta E(298) = \Delta E_{\text{elect}}(0) + \Delta \text{VZPE} + \Delta \Delta E_{\text{vib}}(298) + \Delta E_{\text{rot}}(298) + \Delta E_{\text{trans}}(298)$$

$$\Delta E(0) = \Delta E_{\text{elect}}(0) + \Delta \text{VZPE}$$

$$\Delta G(298) = \Delta H(298) - 298.15 \Delta S(298)$$

dioxide and two nitroso compounds, the difference  $\Delta \text{VZPE}$  in their zero-point energies, the change  $\Delta \Delta E_{\text{vib}}(298)$  between the vibrational energy at room temperature and  $\Delta \text{VZPE}$ , and the differences in the rotational and translations energies,  $\Delta E_{\text{rot}}(298)$  and  $\Delta E_{\text{trans}}(298)$ , respectively, between the dimer and the monomers. The term  $\Delta E(298)$  is often approximated by  $\Delta E(0)$ , that is, only the first two terms for  $\Delta E(298)$  are considered and T-dependent contributions are neglected. The reaction free energy results by addition of the  $-T\Delta S$  term to the reaction enthalpy. We evaluated all of these terms for the formations of the *trans*-isomers of **3**–**5**, and the results are summarized in Table 7.

As expected, the theoretical model dependency of the reaction energies for the dimerizations and the mixed dimer formation is more significant compared to the isomer preference energies. At the highest level, the HNO dimerization is found to be *exothermic* with  $E_{\text{b}} = 14.5$  kcal/mol and inclusion of the VZPE corrections gives  $E_{\text{b}}^{\text{corr}} = 8.0$  kcal/mol. Note that our best value for the dimerization energy of HNO is in close agreement with the best QCISD(T)/QCISD value by Shancke et al.<sup>21</sup> although we used a significantly larger basis set. Alkyl substitution is found to have but a small effect. Our best values for formations of *trans*-**4** and *trans*-**5** are  $E_{\text{b}} = 15.0$  and 15.8 kcal/mol, respectively. Again, including just the VZPE corrections, the diazene dioxide formations are predicted to be *exothermic*,  $E_{\text{b}}^{\text{corr}} = 9.1$  and 10.6 kcal/mol, respectively. The enthalpies  $\Delta H(298)$  for the formations of the *trans*-isomers **3**–**5** are -9.6, -10.5, and -10.0 kcal/mol, respectively, and their magnitudes differ as much as 1.6 kcal/mol from the  $E_{\text{b}}^{\text{corr}}$  values. In 1965, Christie, Frost, and Voisey<sup>45</sup> measured the dimerization of MeNO and EtNO and found enthalpies of -16.0 and -15.0 kcal/mol, respectively, and reaction entropies of -27 and -23 cal/mol K. Experimental data for the

**Table 8. Comparison of Important Bond Lengths in R(O)NN(O)R'**

bond length	isomer	<b>3</b> , H,H	<b>4</b> , H,Me	<b>5</b> , Me,Me
$d(\text{NN})$	<i>trans</i>	1.3566	1.3542	1.3568
	<i>cis</i>	1.3630	1.3628	1.3785
	<i>cis</i> - <i>trans</i>	0.0064	0.0086	0.0217
$d(\text{NO})$	<i>trans</i>	1.2527	1.2534, 1.2628	1.2641
	<i>cis</i>	1.2468	1.2512, 1.2622	1.2570
	<i>cis</i> - <i>trans</i>	-0.0059	-0.0022, -0.0006	-0.0071

<sup>a</sup> All bond lengths in angstroms.

formations of **3** and **4** are not available. The calculated entropy change for formation of **5** deviates drastically from the experimental value, and the absolute dimer formation enthalpies appear to be underestimated by roughly 5 kcal/mol even at the high levels of *ab initio* theory employed here. Considering the great electronic changes associated with the NN bond formation, two  $\sigma$ -lone pairs transformed into a  $\sigma^2\pi^2$  system (*vide infra*), the agreement between theory and experiment is surprisingly good. In the present context, the relative changes of the dimer formation energies are more pertinent than the absolute values, and the relative changes as a function of the number of alkyl groups can reasonably be expected to be more accurate and much less sensitive to the theoretical model (Table 6). The  $\Delta H(298)$  values of  $-10.0 \pm 0.5$  kcal/mol show that the successive introductions of two methyl groups have only a minor effect on the binding energy of the dimer.

Nitroso compounds are intermediates in the reduction of nitro compounds, and their dimerization is clearly *exothermic*. Yet, diazene dioxides are never considered in discussions of RNO<sub>2</sub> reductions.<sup>47</sup> The absence of the diazene dioxides in RNO<sub>2</sub> reductions might reflect a significant kinetic inhibition to this dimer formation or it might involve an impediment of the dimerization by the competing faster combination of RNO with RNHOH to give RN(O)NR, or a high rate of further reduction under the experimental conditions.

#### Structural Characteristics of Diazene Dioxides.

The summary of the MP2(full)/6-31G\*-optimized distances of the isomeric structures in dependence of the number of methyl groups (Table 8) shows that the NN distance always is longer in the *cis* isomer. This difference is minor (and is likely to reflect NO bond dipole repulsion) so long as at least one of the R groups remains hydrogen. A significant isomer dependence occurs otherwise for steric reasons. In the *trans* series, that is, without R-dependent changes in steric interactions, there are virtually no structural consequences associated with the H/Me replacement. The opposite is true for the NO bond distances even though these bonds are generally less sensitive to H/Me replacement.

The most characteristic and frequently pointed out structural feature of the diazene dioxides is the shortness of the NN bond lengths which is clearly indicative of double bond character. The structural relaxations of HNO and RNO upon dimerization provides another important clue to an understanding of the bonding in the dioxides that apparently had been overlooked. With reference to the RNO ground state structure (R = H, Me), dimerization lengthens the NO bonds slightly and *dramatically increases* the  $\angle(\text{R}-\text{N}-\text{O})$  angle. These structural features are fully consistent with the formation of

(47) Review of nitrosobenzene chemistry: Zuman, P.; Shah, B. *Chem. Rev.* **1994**, *94*, 1621.

the 4-center–6-electron  $\pi$  system in the dimer. Formally, the dimer formation can be thought of as a sequence involving the promotion of one  $N_{\sigma}$  lone pair electron into a  $\pi^*$  MO and subsequent  $\sigma$  and  $\pi$  bond formation between the unpaired electrons in the  $N_{sp^2}$  type  $\sigma$ -MO and the  $\pi^*$  MO. The  $\pi$ -MOs in the diazene dioxide greatly resemble the familiar MOs of butadiene. In particular, the  $\pi$ -HOMO contains nodes between N and O atoms while it is *bonding* in the NN region and responsible for the double bond character of the NN bond. The nodal properties of this HOMO also explain the somewhat elongated N–O bond lengths in the dimers compared to HNO.

We considered the  $^3A''$  states of HNO and MeNO to estimate the energy requirements as well as the structural consequences of  $\sigma \rightarrow \pi$  promotion. The optimized structural parameters for the biradicals are underlined in Figures 2 and 3. Note that the conformational preference of  $E_{\text{rot}} = 1.3$  kcal/mol in the biradical state of MeNO is opposite to the one found for the ground state. Most importantly, with reference to these triplet states of the monomers, the dimer formation *lengthens the NO bonds even more*, but it is associated with only a *modest reduction* of the angles  $\angle(R-N-O)$ . The  $\sigma \rightarrow \pi$  excitation leads to a higher  $\sigma$ -character in the nitrogen  $\sigma$  orbitals, and because of this rehybridization the NO bond in the triplet is *shorter* than in the ground state.<sup>48</sup> The strengthening of the NO bond in the triplet state is manifested in an impressive fashion in the vibrational frequencies for the NO stretching vibrations (ca. 2230–2260  $\text{cm}^{-1}$ ) which are about 700  $\text{cm}^{-1}$  higher in the triplet compared to the singlet. Dimerization reduces the frequencies of the normal modes that correspond to the NO stretching vibrations to values in the range of 1625–1800  $\text{cm}^{-1}$ , but they remain significantly higher than in the ground states of RNO (ca. 1490–1560  $\text{cm}^{-1}$ ). At our highest level of calculation, the singlet–triplet gaps are  $E_{1-3} = 20.3$  (HNO) and  $E_{1-3} = 20.7$  kcal/mol (MeNO). These data allow for a rough estimate of about 40 kcal/mol for the upper limit of the activation barrier to dimer formation.

**Charge Distribution and Electrostatic Properties.** A natural bond orbital analysis was carried out to delineate the electronic relaxation upon dimerization. The natural atomic charges (NAC) are given in Figures 2–4. The data for HNO indicate a semipolar NO bond, which can be represented by the resonance forms  $A_M$  and  $B_M$  shown in Figure 5, and that the positive charge formally assigned to N in  $B_M$  actually is delocalized onto the attached H atom. In fact, the  $H \rightarrow N$   $\sigma$  donation more than compensates for the  $N \rightarrow O$  polarization in HNO and N carries a small negative charge. The *replacement of H by the methyl group reduces the excess electron density of the NO bond* and primarily results in a lower electron population of N (NAC = 0.1) while NAC(O) is only marginally affected.

Dimerization to form *trans-3* increases the negative charge of the O atoms by about 0.2 and causes reductions of the N and H atom populations by just about equal amounts. *Dimerization thus increases the polarity of the NO bonds.* The electronic structure of the *cis* isomer is quite similar, although the NO bond polarity increase is slightly less compared to the *trans*-isomer, presumably

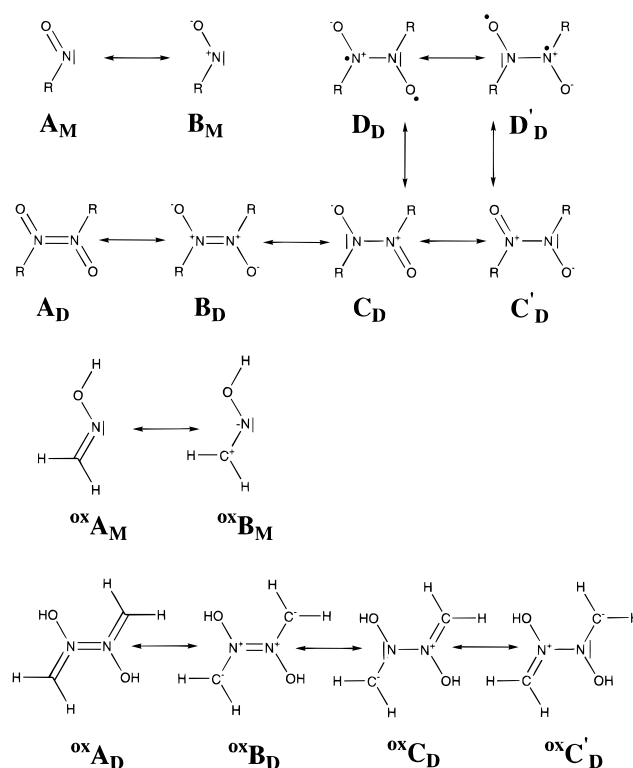


**Figure 5.** Lewis–Kekulé representations of RNO and its dimer diazene dioxide are shown on top. The canonical forms  $D_D$  and  $D'_D$  are the Pauling three-electron bond covalent resonance forms discussed by Harcourt, et al. Lewis–Kekulé representations for the hypothetical dimer formed by NN connection of oximes are shown on the bottom.

to reduce electrostatic repulsion associated with the NO bond dipole moments. Note that the high NO bond polarity of *cis*-diazene dioxides has been exploited for the synthesis of donor–acceptor complexes with TCNE with interesting structural features that suggest the dominance of electrostatic interactions.<sup>49</sup> The *changes* associated with formation of *trans-5* relative to MeNO itself are qualitatively the same as in the case of **3**. Dimerization increases the NAC(O) by 0.22 and causes reductions in the N and Me populations by 0.12 and 0.10, respectively. The *methyl groups lead to a larger increase of the NO bond polarity* as the changes of NAC(O) and NAC(N) both are 0.02 larger compared to the parent system. Aside from steric effects, this feature is likely to contribute to the increase in the *trans* preference energy in going from **3** to **5**. The HNO and MeNO fragments in **4** also show these same electronic relaxation patterns with only minor qualitative differences. Thus, dimer formation always leads to reduced N electron populations. This theoretical finding is in agreement with the experimental results by Lüttke<sup>50</sup> which demonstrate that the thermodynamic stability of the dioxidiazenes correlates with the electron donor ability of the R group.

The increase of the NO bond polarities upon dimerization discussed on the basis of *atomic* properties is clearly evidenced by the *molecular* electrostatic properties given in Table 9. The dipole moments of the *cis*-dimers

(48) Although still considered “extremely rare” (see e.g. Hoffmann, R. *Am. Sci.* **1995**, 309.), molecules with shorter bond lengths in excited states than in their ground states are actually quite common in situations where the  $n \rightarrow \pi^*$  excitation is associated with rehybridization as in the case discussed here and numerous examples can be found in Herzberg’s books on molecular spectroscopy.

(49) Blackstone, S. C.; Poehling, K.; Greer, M. L. *J. Am. Chem. Soc.* **1995**, *117*, 6617, and references cited therein.

(50) (a) Lüttke, W. *Z. Elektrochem.* **1957**, *61*, 302, 976. (b) Kaissler, V. v.; Lüttke, W. *Z. Elektrochem.* **1959**, *63*, 614. (c) See also: Gowenlock, B. G.; Lüttke, W. *Quart. Rev. (London)* **1958**, *12*, 321.

**Table 9. Dipole and Quadrupole Moments of the  $^1A'$  and  $^3A''$  States of RNO (R = H, Me) and of the Ground States of Diazene Dioxides 3–5**

property	HNO, $^1A'$ $C_s$	HNO, $^3A''$ $C_s$	<i>trans</i> -3 $C_{2h}$	<i>cis</i> -3 $C_{2v}$	H <sub>2</sub> C=NOH $C_s$
$\mu$	1.79	2.39	0	5.55	0.24
$q_{xx}$	-11.04	-10.19	-23.66	-22.63	-11.55
$q_{yy}$	-11.75	-0.94	-25.96	-25.55	-19.30
$q_{zz}$	-10.46	-11.60	-22.59	-18.36	-18.93
$q_{xy}$	-1.52	-1.48	-8.01	0.00	-1.56
property	MeNO, $^1A'$ $C_s, \tau = 180^\circ$	MeNO, $^3A''$ $C_s, \tau = 180^\circ$	MeNO, $^1A'$ $C_s, \tau = 0^\circ$	MeNO, $^3A''$ $C_s, \tau = 0^\circ$	
$\mu$	2.28	2.95	2.32	2.95	
$q_{xx}$	-18.41	-18.25	-18.16	-18.38	
$q_{yy}$	-19.16	-17.40	-19.29	-17.28	
$q_{zz}$	-16.64	-17.59	-16.66	-17.59	
$q_{xy}$	0.33	0.00	0.30	0.02	
property	<i>trans</i> -4 $C_s, \tau = 180^\circ$	<i>trans</i> -4 $C_s, \tau = 0^\circ$	<i>cis</i> -5 $C_{2v}, \tau = 0^\circ$	<i>cis</i> -5 $C_2$	<i>trans</i> -5 $C_{2h}, \tau = 0^\circ$
$\mu$	1.05	0.88	6.46	6.40	0
$q_{xx}$	-22.83	-22.56	-34.76	-34.68	-35.48
$q_{yy}$	-39.00	-39.12	-34.94	-34.94	-37.19
$q_{zz}$	-28.55	-28.60	-38.56	-38.31	-34.66
$q_{xy}$	-2.76	-2.34	0.00	-0.27	-9.59

<sup>a</sup> MP2(full)/6-31G\* level. Dipoles in Debye and quadrupoles in Debye Å. <sup>b</sup> In all cases:  $q_{xz} = q_{yz} = 0$ .

**3** and **5** are 5.4 and 6.4 Debye, respectively, at the correlated level.<sup>51</sup> Most importantly, the *dipole moments of the dimers greatly exceed the dipole moments resulting from appropriate vector superposition of the dipole moments of the unperturbed monomers*. In the *trans*-structures, the high magnitudes of the quadrupole moment tensor elements  $q_{ij}$  provide similar and compelling evidence.

The NO bond polarity increase upon dimerization effectively promotes an electron density transfer to the most electronegative element. We consider this charge transfer as the driving force for diazene dioxide formation. Corroborating evidence is provided by analysis of the ethylenedione formation. Haddon and co-workers<sup>52</sup> studied the dimerization of CO and found it to be greatly endothermic. The ground state electron configuration of C<sub>2</sub>O<sub>2</sub> contains two orthogonal 4-center–5-electron  $\pi$ -systems which give rise to the  $^3\Sigma_g^-$  ground state and a  $^1\Sigma_g^+$  excited state with similar geometries and electronic structures. The triplet state of C<sub>2</sub>O<sub>2</sub> is described adequately by a single determinant wavefunction, and we carried out an NBO analysis of this state (Figure 6). The NBO analysis indicates a reduction of the CO bond polarity and charge transfer to the *less electronegative* element in this *endothermic* C<sub>2</sub>O<sub>2</sub> formation.

The NBO analysis suggests that the electronic structure of the dimer might best be represented by the degenerate set of resonance forms **C<sub>D</sub>** and **C<sub>D</sub>'** (Figure 5). The resonance forms **A<sub>D</sub>** and **B<sub>D</sub>** formally result from N=N bond formation using **A<sub>M</sub>** or **B<sub>M</sub>**, and it is these two

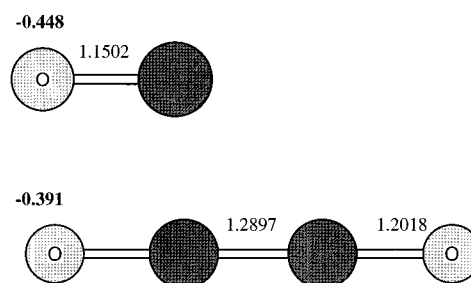


**Figure 6.** MP2(full)/6-31G\* optimized structures of CO and C<sub>2</sub>O<sub>2</sub>,  $^3\Sigma_g^-$ . The MP2(full)/6-31G\* NBO atomic charges are given in bold.

resonance forms that formally account for the double bond character of the NN bond. The notation **A<sub>D</sub>** should not be dismissed because it “violates the octet rule”; this notation is a rather useful notation to describe the 4-center–6-electron  $\pi$ -system which does indeed provide double bond character to all three bonds. The results of the NBO analysis agree with the conclusions made by Harcourt, Skrezenek, and Gowenlock<sup>53</sup> in their ab initio valence-bond studies of the *cis* and *trans* isomers of **3** at the STO-6G level and using standard structures. Their valence-bond (VB) analysis suggests that the so-called Pauling three-electron bond covalent–ionic resonance forms **D<sub>D</sub>** and **D'<sub>D</sub>** also are important. Note that the results of the VB study provide strong evidence in favor of the increased-valence structure representation **A<sub>D</sub>**.

The electronic structure analysis provides a simple explanation as to why the nitroso compound undergoes the formation of the NN connected dimers rather than the oxime (bottom in Figure 5). For the parent system, the nitroso form H<sub>3</sub>CN=O is *less stable* than the oxime form H<sub>2</sub>C=NOH by 10.2 kcal/mol.<sup>54</sup> Dimer formation leading to the *O,O'*-tautomer (**oxA<sub>D</sub>**–**oxC'<sub>D</sub>**) or the *C,C'*-tautomer (**A<sub>D</sub>**–**C'<sub>D</sub>**), respectively, increases the electron density on oxygen while it results in a *polarization*

(51) The earlier estimate of 8.7 Debye obtained at the RHF/4-31G level by Minato et al. greatly exceeds the value computed here at the correlated level. Note that the deviation is of about the same magnitude as for nitrosomethane for which a comparison between the experimental and theoretical dipole moments was made.

(52) (a) Haddon, R. C. *Tetrahedron Lett.* **1972**, 37, 3897. (b) Haddon, R. C.; Poppinger, D.; Radom, L. *J. Am. Chem. Soc.* **1975**, 97, 1645, and references therein. (c) Raine, G. P.; Schaefer, H. F.; Haddon, R. C. *J. Am. Chem. Soc.* **1983**, 105, 194, and references therein. (d) MP2(full)/6-31G\* data:  $E(\text{CO}) = -113.028180$  au,  $VZPE(\text{RMP2}) = 3.04$  kcal/mol; linear singlet C<sub>2</sub>O<sub>2</sub> [denoted ( $^1\Sigma_g^+$ ) in ref b],  $d(\text{CC}) = 1.2930$  Å,  $d(\text{CO}) = 1.2089$ ,  $q^{\text{NBO}}(\text{O}) = -0.355$ ,  $E(\text{RMP2}) = -225.942805$  au,  $VZPE(\text{RMP2}) = 9.01$  kcal/mol,  $\text{NIMAG} = 1$  (1543 cm<sup>-1</sup>,  $\pi_g$ );  $E_{\text{dim}} = 71.3$  kcal/mol; linear triplet C<sub>2</sub>O<sub>2</sub>,  $d(\text{CC}) = 1.2897$  Å,  $d(\text{CO}) = 1.2018$ ,  $q^{\text{NBO}}(\text{O}) = -0.391$ ,  $E(\text{UMP2}) = -225.961007$  au,  $VZPE(\text{UMP2}) = 8.66$  kcal/mol,  $\text{NIMAG} = 0$ ,  $E_{\text{dim}} = 59.8$  kcal/mol.

(53) Harcourt, R. C.; Skrezenek, F. L.; Gowenlock, B. G. *J. Mol. Struct. (Theochem)* **1993**, 284, 87.

(54) The catalytic rearrangement of MeNO into thermodynamically preferred H<sub>2</sub>C=NOH has been reported: Duxbury, G.; Percival, R. M.; Devoy, D.; Mahmoud, M. R. M. *J. Mol. Spectrosc.* **1988**, 132, 380.

reversal for the C atom in the case of the oxime. It is the advantage associated with accumulation of excess charge on the oxygens that provides a simple, yet compelling, explanation for the preferred formation of the dioxide **A** instead of the diol **B**. In fact, searches of the Cambridge Crystallographic Database for *O,O'*-tautomers and derived ethers did not result in any hit and indicate, furthermore, that apparently no crystal structures are known to date of dimers formed between an oxime (or oxime ether) and a nitroso compound. Tautomers **C** and **D** are disadvantaged for the same reason.

**Acknowledgment** is made to the donors of the Petroleum Research Fund, administered by the American Chemical Society, to the MU Research Board, and to the MU Department of Chemistry for partial support of this research. X-ray and NMR equipment were funded by the National Science Foundation. We wish

to express our sincere appreciation to Dr. Guo Wei for NMR expertise and help. We thank the Campus Computing Center for a generous allowance of computer time and Steve Meyer for system management.

**Supporting Information Available:** Four tables with computed vibrational frequencies and their infrared intensities and assignments (6 pages). This material is contained in libraries on microfiche, immediately follows this article in the microfilm version of the journal, and can be ordered from the ACS; see any current masthead page for ordering information. Atomic coordinates, structure factors, positional parameters, and anisotropic thermal parameters for *trans*-dimeric 2-chloro-2-methyl-3-nitrosobutane were deposited with the Cambridge Crystallographic Data Centre. This material can be obtained from the Director, Cambridge Crystallographic Data Centre, 12 Union Road, Cambridge, CB2 1EZ, UK.

JO950783K